



ELSEVIER

Contents lists available at ScienceDirect

## Comptes Rendus Chimie

www.sciencedirect.com



Preliminary communication/Communication

# Synthesis, crystal structures and spectroscopic properties of two new organotin(IV) complexes and their antiproliferative effect against cancerous and non-cancerous cells



Yip-Foo Win<sup>a,\*</sup>, Chen-Shang Choong<sup>a</sup>, Jia-Chin Dang<sup>a</sup>,  
 Muhammad Adnan Iqbal<sup>b</sup>, Ching Kheng Quah<sup>c</sup>, Sharmila Rajeswari Kanuparth<sup>d</sup>,  
 Rosenani A. Haque<sup>b</sup>, Mohamed B. Khadeer Ahamed<sup>d</sup>, Siang-Guan Teoh<sup>b,\*</sup>

<sup>a</sup> Department of Chemical Science, Faculty of Science, Universiti Tunku Abdul Rahman, Perak Campus, Jalan Universiti, Bandar Barat, 31900 Kampar, Perak, Malaysia

<sup>b</sup> School of Chemical Sciences, Universiti Sains Malaysia, 11800 USM, Penang, Malaysia

<sup>c</sup> X-ray Crystallography Unit, School of Physics, Universiti Sains Malaysia, 11800 USM, Penang, Malaysia

<sup>d</sup> EMAN Research and Testing Laboratory, School of Pharmaceutical Sciences, Universiti Sains Malaysia, 11800 USM, Penang, Malaysia

## ARTICLE INFO

## Article history:

Received 2 May 2014

Accepted after revision 3 June 2014

Available online 13 January 2015

## Keywords:

Organotin(IV) carboxylate complexes

Cytotoxicity

HCT 116

MCF-7

K562

3T3-L1

## ABSTRACT

Cancer has become a leading cause of death worldwide, which is responsible for 7.6 million cancer deaths according to GLOBOCAN survey conducted in 2008. The exploration of *cis*-platin analogues (carboplatin, lobaplatin, nedaplatin, oxaliplatin) and their incorporation to the treatment of cancer patients has further led interest in exploring metal-based anticancer drugs. The current study describes the synthesis of two new tetra-coordinated mono- and tetranuclear organotin(IV) carboxylate complexes and their *in vitro* anticancer studies. Each one of the complexes (**1–2**) has been characterized by analytical (micro- and gravimetric analysis) and spectroscopic (FTIR, <sup>1</sup>H, <sup>13</sup>C, <sup>119</sup>Sn-NMR) techniques. Furthermore, molecular structures of **1** and **2** were elucidated using X-ray crystallography. The characterization data showed that the coordination took place via oxygen atoms from the carboxylate anions to generate **1** as an organodistannoxane dimer and **2** as a mononuclear complex. Exceptionally, the NMR spectroscopic and X-ray crystallographic study showed that acetone molecules also took part in crystallizing **2**. Both complexes were tested against three cancerous (colon cancer HCT 116, breast cancer MCF 7, leukemia K562) and one non-cancerous (3T3-L1) cell lines. Both complexes showed same IC<sub>50</sub> value (0.2 μM) against HCT 116, whereas for the other two cancer cell lines (MCF 7 and K562) and a normal cell line (3T3-L1), **2** showed results better than **1**. Importantly, the complexes showed exceptional activity against MCF 7 and K562 cell lines and the IC<sub>50</sub> values were calculated in nanomoles (MCF 7, IC<sub>50s</sub> = 86.5 and 53.4 nM; K 562, IC<sub>50s</sub> = 22.9 and 49.6 nM for **1** and **2**, respectively). Both, **1** and **2**, showed IC<sub>50</sub> values many times better than the standard drugs (5-FU, Tamoxifen, betulinic acid and *cis*-platin) used. Compared to cancerous cell lines, the complexes showed mild toxicity against normal cells (3T3-L1). Overall, two remained relatively effective.

© 2014 Académie des sciences. Published by Elsevier Masson SAS. All rights reserved.

\* Corresponding authors. School of Chemical Sciences, Universiti Sains Malaysia, 11800 USM, Penang, Malaysia.

E-mail addresses: ppsk1@yahoo.com (Y.-F. Win), sgteoh@usm.my (S.-G. Teoh).

## 1. Introduction

Beside the fact that most of the anticancer drugs placed in the market are organic compounds [1], the metal-based chemotherapeutic drugs are now becoming popular because of their different mechanisms of action compared with organic chemotherapeutic agents [1–3]. *Cis*-platin and recently, its new analogues (carboplatin, lobaplatin, oxaliplatin and nedaplatin) are being marketed to cure cancer patients. This has further led interest in the field of metal-based anticancer drugs. With this recent development, researchers are now interested to explore the biological significance of either the borderline or non-transition metals due to their lower toxicity compared to transition metals. This is also evident by recently compiled reviews [3,4].

Tin is a non-transition and biocompatible metal [5–7] and its complexes have shown significant antibacterial properties [8–22]. However, tin complexes have been rarely studied against cancer [12,23–28]. The current study is an effort to further explore this area of research.

The organotin(IV) complexes show interesting coordination geometries as well as structural diversity, which could expand from simple, monomeric to polymeric structures [8,29–35]. This gives biological significance to the tin complexes where their coordination motives and geometry can be monitored. In addition, based on well-documented X-ray crystallographic study, in some cases, the participation of solvent molecules such as water, acetone and methanol in organotin(IV) complexes influences the overall structure of organotin(IV) complexes including its packing which may enhance their water solubility [31,32,34,36].

In this paper, we report the synthesis and structural characterization of organotin(IV) carboxylate complexes (**1–2**) derived from 5-amino-2-chlorobenzoic acid (**HL**) and their *in vitro* anticancer studies against three cancerous and one non-cancerous (normal) cell lines.

## 2. Experimental

### 2.1. General and instrumental

All the reagents, starting materials as well as the solvents were purchased commercially and were used without any further purification. Elemental C, H and N analyses were carried out on a Perkin-Elmer 2400 CHN Elemental Analyzer. Tin was determined gravimetrically by igniting a known quantity of each complex to SnO<sub>2</sub>. The melting points were determined in an open capillary and were uncorrected. The infrared spectra were recorded using a Perkin-Elmer System 2000 FTIR Spectrophotometer as a KBr disc in the frequency range of 4000–400 cm<sup>-1</sup>. The spectra for <sup>1</sup>H, <sup>13</sup>C and <sup>119</sup>Sn-NMR were recorded on a Joel JNM-ECX 400 FT-NMR Spectrometer using deuterated *d*<sub>6</sub>-DMSO as the solvent and tetramethylsilane, TMS as the internal standard.

Single crystal X-ray diffraction data were collected on Bruker APEX II or APEX II Duo CCD area-detector diffractometer operating at 50 kV and 30 mA using Mo

K $\alpha$  radiation ( $\lambda = 0.71073 \text{ \AA}$ ). Diffraction data for complexes **1–2** were collected with the Oxford Cryosystem Cobra low temperature attachment at 100 K [37]. Data collection and reduction were performed using the APEX2 and SAINT software. The SADABS software was used for absorption correction. All structures were solved by direct method and refinement was carried out by the full-matrix least-squares technique on  $F^2$  using SHELXTL package [38]. All non-hydrogen atoms were refined anisotropically whereas hydrogen atoms were refined isotropically. All N-bound H atoms were located in difference Fourier maps and fixed at their found positions and refined with  $U_{\text{iso}}(\text{H}) = 1.2 U_{\text{eq}}(\text{N})$ . The hydrogen atoms bound to C atoms were positioned geometrically with  $U_{\text{iso}}(\text{H}) = 1.2$  or  $1.5 U_{\text{eq}}(\text{C})$ . A rotating-group model was applied for the methyl groups.

### 2.2. 5-Amino-2-chlorobenzoic acid, HL

The parent acid, 5-amino-2-chlorobenzoic acid, **HL** was purchased from Acros Organics and was used without any further purification. FTIR as KBr disc (cm<sup>-1</sup>): selected data:  $\nu(\text{OH})$  2500–3400,  $\nu(\text{COO})_{\text{as}}$  1624,  $\nu(\text{COO})_{\text{s}}$  1371,  $\Delta\nu = 253$ . <sup>1</sup>H-NMR (ppm) (*d*<sub>6</sub>-DMSO):  $\delta$ : benzene protons 6.64 (dd, 2.4 Hz, 8.6 Hz, 1H); 6.91 (d, 3.0 Hz, 1H); 7.06 (d, 9.2 Hz, 1H). <sup>13</sup>C-NMR (ppm) (*d*<sub>6</sub>-DMSO):  $\delta$ : benzene carbons 115.8, 117.6, 118.1, 131.3, 131.98, 147.9; COO 166.9.

### 2.3. Preparation of sodium salt (HL-Na)

The sodium salt of the acid was obtained by heating under reflux a 1:1 molar mixture of sodium hydroxide, NaOH and 5-amino-2-chlorobenzoic acid in ethanol (50 mL) for two hours. After few days, white precipitates were obtained. Sodium salt of 5-amino-2-chlorobenzoic acid: FTIR as KBr disc (cm<sup>-1</sup>) selected data:  $\nu(\text{COO})_{\text{as}}$  1565,  $\nu(\text{COO})_{\text{s}}$  1387,  $\Delta\nu = 178$ .

### 2.4. Synthesis of complexes

#### 2.4.1. Preparation of $[\{5\text{-NH}_2\text{-2-Cl-C}_6\text{H}_3\text{COO}(\text{C}_4\text{H}_9)_2\text{Sn}\}_2\text{O}]_2$ (**1**)

Complex **1** was obtained by heating under reflux a 1:1 molar mixture of dibutyltin(IV) oxide (1.50 g, 6 mmole) and 5-amino-2-chlorobenzoic acid (1.03 g, 6 mmole). The reaction was carried out in a mixture of ethanol/toluene (1:4, 60 mL) for three hours. A clear transparent solution was isolated by filtration and kept in a bottle. After few days, colorless crystals (2.17 g, 88.0% yield) were collected. Melting point: 200–202 °C. Analysis for C<sub>60</sub>H<sub>92</sub>N<sub>4</sub>O<sub>10</sub>Cl<sub>4</sub>Sn<sub>4</sub>: 42.58; H, 6.66; N, 3.76; Sn, 27.11%. Calculated for C<sub>60</sub>H<sub>92</sub>N<sub>4</sub>O<sub>10</sub>Cl<sub>4</sub>Sn<sub>4</sub>: C, 43.78; H, 5.63; N, 3.41; Sn, 28.84%. FTIR as KBr disc (cm<sup>-1</sup>):  $\nu(\text{COO})_{\text{as}}$  1637, 1600,  $\nu(\text{COO})_{\text{s}}$  1281, 1342,  $\Delta\nu = 356, 258$ ;  $\nu(\text{O-Sn-O})/\nu(\text{Sn-O-Sn})$  629,  $\nu(\text{Sn-C})$  556,  $\nu(\text{Sn-O})$  436. <sup>1</sup>H-NMR (ppm) (*d*<sub>6</sub>-DMSO):  $\delta$ : benzene protons 6.54 (d, 6.8 Hz, 8H); 6.98 (d, 8.2 Hz, 4H); butyl, CH<sub>3</sub> 0.75 (t, 7.3 Hz, 12H), 0.79 (t, 7.4 Hz, 12H); CH<sub>2</sub> 1.15–1.29 (m, 32H); CH<sub>2</sub> 1.43–1.60 (m, 16H). <sup>13</sup>C-NMR (ppm) (*d*<sub>6</sub>-DMSO):  $\delta$ : benzene carbons 116.1, 117.6, 130.2, 13.0, 148.0; butyl 14.0, 14.1, 26.2, 26.9, 27.0, 27.4; COO 172.1. <sup>119</sup>Sn-NMR (ppm) (*d*<sub>6</sub>-DMSO):  $\delta$ : -185.7, -230.8.

### 2.4.2. Preparation of {5-NH<sub>2</sub>-2-Cl-C<sub>6</sub>H<sub>3</sub>COO(C<sub>6</sub>H<sub>5</sub>)<sub>3</sub>Sn}<sub>2</sub>(CH<sub>3</sub>)<sub>2</sub>CO (2)

The title complex was obtained by heating under reflux a 1:1 molar mixture of triphenyltin(IV) hydroxide (1.47 g, 4 mmole) and 5-amino-2-chlorobenzoic acid (0.69 g, 4 mmole) in acetone (50 mL) for two hours. A clear solution was isolated by filtration and kept in a bottle. After few days, transparent crystals (1.56 g, 81.0% yield) were collected. Melting point: 127–129 °C. Analysis for C<sub>53</sub>H<sub>46</sub>N<sub>2</sub>O<sub>5</sub>Cl<sub>2</sub>Sn<sub>2</sub>: C, 57.46; H, 4.17; N, 2.69; Sn, 20.01%. Calculated for C<sub>53</sub>H<sub>46</sub>N<sub>2</sub>O<sub>5</sub>Cl<sub>2</sub>Sn<sub>2</sub>: C, 57.91; H, 4.22; N, 2.55; Sn, 21.59%. FTIR as KBr disc (cm<sup>-1</sup>): ν(COO)<sub>as</sub> 1623, ν(COO)<sub>s</sub> 1355, Δν = 268; ν(Sn–O) 453. <sup>1</sup>H-NMR (ppm) (d<sub>6</sub>-DMSO): δ: phenyl protons 7.36–7.42 (m, 18H); 7.72–7.90 (m, 12H); benzene 6.48 (dd, 3.0 Hz, 8.6 Hz, 2H); 6.68 (d, 3.1 Hz, 2H); 6.93 (d, 8.6 Hz, 2H); (CH<sub>3</sub>)<sub>2</sub>CO 2.04 (s, 6H). <sup>13</sup>C-NMR (ppm) (d<sub>6</sub>-DMSO): δ: phenyl carbons C<sub>ipso</sub> 143.4, C<sub>ortho</sub> 136.7 (46.0 Hz), C<sub>meta</sub> 128.4 (69.0 Hz), C<sub>para</sub> 128.7; benzene 115.4, 116.4, 117.0, 129.4, 130.6, 147.7; (CH<sub>3</sub>)<sub>2</sub>CO 30.0, 207.7; COO 170.2. <sup>119</sup>Sn-NMR (ppm) (d<sub>6</sub>-DMSO): δ: –260.8.

### 2.5. In vitro anticancer studies

The synthesized compounds were dissolved in DMSO to obtain 10 mM stock solution. For experiment, the compounds were diluted in the indicated culture medium at the indicated concentrations in each test. DMSO (0.1%) was used as a negative control. Source of cell lines, culture conditions, preparation of cell culture and MTT assay were performed according to our previously reported procedure

for these cell lines [39–42]. The details of cell culture conditions, preparation of cell culture and MTT assay procedure has been additionally provided in supplementary file.

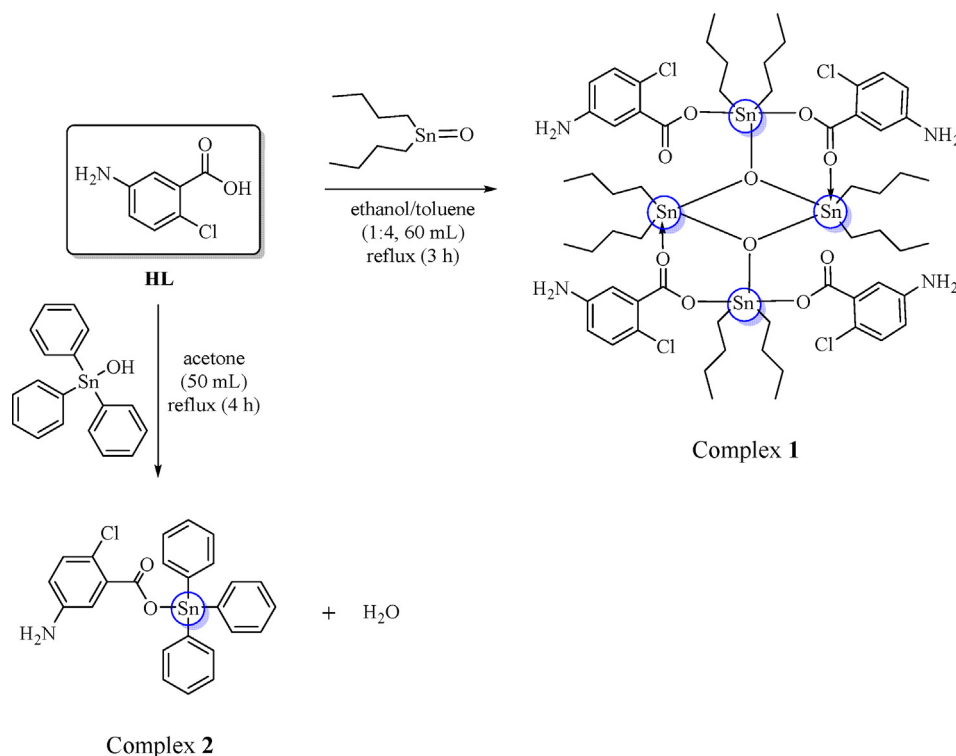
## 3. Results and discussion

### 3.1. Synthesis

In this study, complexes **1–2** have been obtained in solid state. Complexes **1–2** gave a sharp melting points (with a range of less than 3 °C) indicating the isolation of fairly pure complexes. Synthesis of complexes **1–2** has been provided in [Scheme 1](#). The micro-elemental analyses for data obtained were in agreement with the predicted formula for complexes **1–2**. Based on the micro-elemental analysis, it was believed that acetone molecule was present in complex **2** which acted as a solvate molecule [31,32,34,36].

### 3.2. Characterization by FTIR spectroscopy

The synthesized complexes (**1–2**) as well the starting materials (**HL** and **HL-Na**) were preliminarily characterized by FTIR to observe the possible spectral changes in complexes than compared to reactants. [Fig. 1](#) represents the overlay spectra of reactants (**HL** and **HL-Na**) and complexes (**1–2**), highlighting the observable changes. The ν(O–H) bands of the acid, **HL** was absent in the infrared spectra of salt and complexes **1–2** which indicated the deprotonation and possible coordination of the carboxylate



**Scheme 1.** (Color online.) Synthesis of tin complexes **1** and **2**.

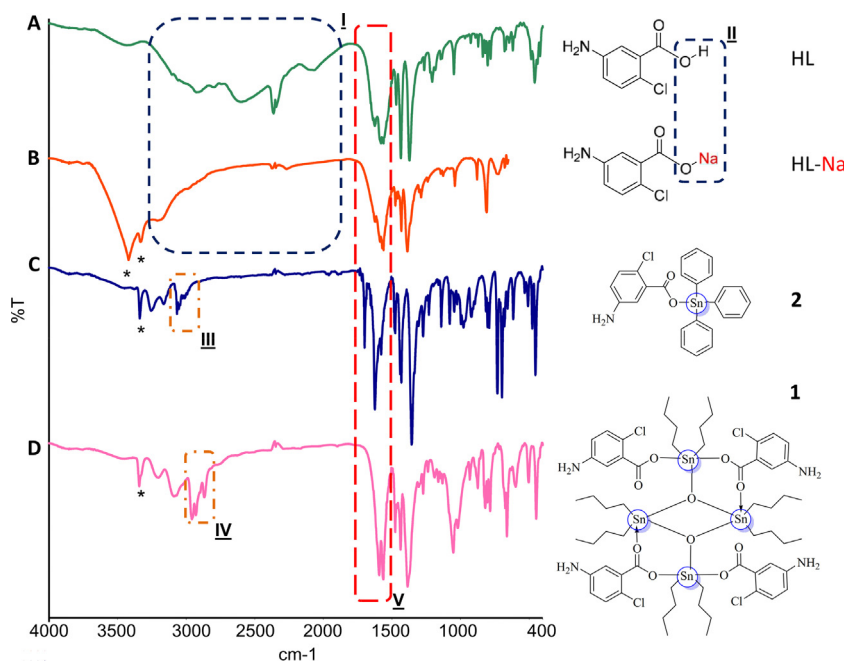


**Fig. 1.** (Color online.) FTIR spectral features of **HL**, **HL-Na**, **1** and **2**. Spectrum A (for **HL**) shows that a broad vibrational band ( $2500\text{--}3400\text{ cm}^{-1}$  for  $\text{COOH}$ ) vanished in spectrum B (for **HL-Na**) due to the replacement of proton with sodium ion indicating the possible salt formation. In spectrum B two “\*” symbols as enhanced vibrational bands ( $3332$  and  $3422\text{ cm}^{-1}$ ) indicated the presence of primary amine. These vibrations remained suppressed in **HL**, perhaps due to the presence of either intermolecular H-bonding or overlapped by  $\text{COOH}$  vibrations. Also, changes in the patterns of these  $\text{NH}_2$  vibrations in the complexes **1** and **2** might be due to stronger intermolecular H-bonding as can be seen in the crystal packing of these complexes (Supplemental). Furthermore, in spectrum C, appearance of highlighted vibrations **III** ( $3000\text{--}3100\text{ cm}^{-1}$ ) and in D, **IV** ( $2800\text{--}3000\text{ cm}^{-1}$ ) verified the enhanced aromatic rings ( $\text{C-H}_{\text{arom}}$ ) in **1** and incorporation of alkyl groups ( $\text{C-H}_{\text{alkyl}}$ ) in **2**, respectively. In all the spectra (A–D), the highlighted region **V** indicates the observed changes for  $\nu(\text{COO})_{\text{as}}$  before and after coordination as described in the text of the article.

anion with the metal cation [43]. In addition, complex **2** revealed that the  $\nu(\text{COO})_{\text{as}}$  shifted to a lower wavenumber compared to the acid, **HL** which signified that the coordination took place via the oxygen atoms of the carboxylate anion. From the infrared spectrum of **1**, the first  $\Delta\nu$  value ( $356\text{ cm}^{-1}$ ) was larger than the  $\Delta\nu$  value of the sodium salt while the second  $\Delta\nu$  value ( $258\text{ cm}^{-1}$ ) was comparable to the sodium salt ( $194\text{ cm}^{-1}$ ) indicating a pair of carboxylate anions coordinated in monodentate manner while another pair coordinated in bidentate manner [44].

For complexes derived from triphenyltin(IV) carboxylate,  $\Delta\nu$  greater than  $200\text{ cm}^{-1}$  would be expected for the monodentate bonding carboxylate anions [45]. Hence, the carboxylate anion in complex **2** would be expected to bond to the tin(IV) atom in monodentate manner since the  $\Delta\nu$  is above  $200\text{ cm}^{-1}$ . For further evidence of the coordination to tin(IV) atom via oxygen atoms revealed by the presence of the  $\nu(\text{O-Sn-O})/\nu(\text{Sn-O-Sn})$  and  $\nu(\text{Sn-O})$  stretching bands in the spectra of **1–2**.

### 3.3. Characterization by $^1\text{H}$ , $^{13}\text{C}$ , $^{119}\text{Sn}$ -NMR spectroscopies

The  $^1\text{H}$ -NMR spectra of **1–2** exhibited similarities to the acid, **HL**. The only exceptional differences were in the upfield regions of the  $^1\text{H}$ -NMR spectrum of **1** which showed the signals of the butyl protons of the organotin(IV) at  $0.83\text{ ppm}$  and in the range of  $0.75\text{--}1.60\text{ ppm}$ . Whereas for **2**, the resonances appeared as two well separated sets of multiplets in the regions centering

around  $\delta \approx 7.39$  and  $7.81\text{ ppm}$  (downfield) with the integration values of 9:6 respectively, ascribed to the aromatic protons of the phenyl group [46]. Furthermore, based on the  $^1\text{H}$ -NMR spectral studies of **2**, the proton resonances originating from the acetone molecule occurred at  $\delta = 2.04\text{ ppm}$  and based on the integration, only one acetone molecule was expected to be present in **2**.

Evidences of the formation of the complexes were further observed in the  $^{13}\text{C}$ -NMR spectra. The  $^{13}\text{C}$ -NMR spectra of complexes **1–2** showed that the  $\delta(\text{COO})$  signals shifted to the downfield region compared to that of the acid, **HL** indicating the carboxylate anion were bonded to tin(IV) atoms. Complex **1** is derivative of organodistannoxane dimer types which exhibited two sets of signals corresponding to the butyl groups in the  $^{13}\text{C}$ -NMR spectra. These two sets of signals were assigned to the butyl groups linked to the exo- and endocyclic tin(IV) atoms, respectively [47]. Complex **2** revealed the chemical shifts of the  $\delta(^{13}\text{C})_{\text{ipso}}$  at  $143.4\text{ ppm}$  indicative of a penta-coordinated tin(IV) atom thus indicating that the tin(IV) atom in complex **2** was five-coordinated and has a trans-trigonal bipyramidal geometry [48–50]. In addition, in  $^{13}\text{C}$ -NMR spectrum of **2** the signals due to the presence of acetone molecule were located at  $\delta = 30.0$  and  $207.7\text{ ppm}$ .

The  $\delta(^{119}\text{Sn})$  values of the four-coordinated complexes fall in the range between  $+200$  to  $-60\text{ ppm}$ ; the five-coordinated complexes between  $-90$  to  $-190\text{ ppm}$  and the six-coordinated complexes between  $-210$  to  $-400\text{ ppm}$  [51]. The organodistannoxane dimer type complexes

usually exhibit two well resolved  $\delta(^{119}\text{Sn})$  signals (complex **1** =  $-185.3, -230.8$  ppm). Based on the  $^{119}\text{Sn}$ -NMR spectra, a pair of tin(IV) atoms were five-coordinated and another pair of tin(IV) atoms were six-coordinated in complex **1**. Normally, the  $\delta(^{119}\text{Sn})$  value of triphenyltin(IV) complexes lie in the range between  $-180$  to  $-260$  ppm was believed to be five-coordinated and in the distorted trigonal bipyramid geometry [Ph<sub>3</sub>SnX•L (L is a monodentate ligand)]. Complex **2** showed that the  $\delta(^{119}\text{Sn})$  value at  $-260.88$  ppm which lies slightly upfield in the range of  $-180$  to  $-260$  ppm indicated the tin(IV) atom was penta-coordinated and possessed a trans-trigonal bipyramid geometry [49,50]. From the  $^{119}\text{Sn}$ -NMR study, the acetone molecule (coordinating solvent) was expected to be coordinated to the tin(IV) atom in complex **2** resulting the tin(IV) atom being penta-coordinated.

### 3.4. Characterization by X-ray crystallography

#### 3.4.1. Structural elucidation of complex 1

Single crystal X-ray determination revealed that the crystal system of complex **1** is triclinic with space group *P* $\bar{1}$  and unit cell parameters  $a = 12.2010(6)$  Å,  $b = 12.2891(6)$  Å,  $c = 13.7860(7)$  Å,  $\alpha = 108.029(1)^\circ$ ,  $\beta = 95.744(1)^\circ$  and  $\gamma = 107.168(1)^\circ$ . The summary of the crystallography data of **1** is shown in Table 1 while the selected bond lengths (Å) and angles ( $^\circ$ ) are listed in Table 2. The hydrogen bond geometry (Å,  $^\circ$ ) is given in Table 3. Fig. 2 represents the molecular structure of **1** with its numbering scheme while the molecular packing diagram is depicted in Fig. 1S.

The core geometry of **1** consists of a centrosymmetric, planar, four-membered Sn<sub>2</sub>O<sub>2</sub> unit with the Sn(1)–O(3)–Sn(1A) and O(3)–Sn(1)–O(3A) angles of  $106.65(8)^\circ$  and  $73.35(9)^\circ$  respectively, as observed from the related structure. The Sn<sub>2</sub>O<sub>2</sub> unit was found to be connected to a pair of exocyclic Sn atoms via the bridging oxygen atoms such that the oxygen atoms [O(3) and O(3A)] were tri-coordinated. The

exocyclic tin atom, Sn(2), formed four primary bonds: one to the O(3) atom, one to the carboxylic oxygen atoms, O(4) and two to the tin-bound butyl groups. The endocyclic Sn(1) tin atom was also penta-coordinated and existed in a distorted trigonal bipyramid geometry, with the atoms C(15), C(19), O(3), O(3A) and O(1). Based on the crystal structure of **1**, the Sn(2A) tin atom was exocyclic and had a similar coordination mode to Sn(2) whereas the Sn(1A) tin atom was similar to Sn(1). The chloro- and amine groups did not participate in the coordination to the Sn centres and were directed away from the central unit.

In the crystal structure, the molecules are linked to form a two-dimensional network (Fig. S1) parallel to the (1  $\bar{1}$  0) by C–H...O and N–H...O hydrogen bonds (Table 3).

Based on the spectroscopy studies, it was expected that a pair of carboxylate anions is coordinated in monodentate manner whereas the other pair of carboxylate anions is coordinated in bidentate manner. However, based on the crystallography structure studies of the **1**, all the four carboxylate ligands were found to be connected to each of the exo- and endocyclic Sn(IV) atoms through one oxygen atom of the carboxylate anions. From this study, it has been confirmed that a new type of organodistannoxane dimer has been found and characterized where all the carboxylate anions are bonded in monodentate manner resulting a pair of tin(IV) atoms are tetra-coordinated and another pair of tin(IV) atoms are penta-coordinated.

#### 3.4.2. Structural elucidation of complex 2

Complex **2** was isolated as a colorless single crystals and the structure of the complex was postulated and determined by single crystal X-ray crystallographic technique. Our X-ray study revealed that the crystal system of **2** is orthorhombic, with space group *Pbcn* and unit cell parameters  $a = 14.6013(3)$  Å,  $b = 20.2960(5)$  Å,  $c = 15.8675(4)$  Å;  $\alpha = \beta = \gamma = 90^\circ$ . The molecular structure of **2** with atomic labeling is depicted in Fig. 3. The summary

**Table 1**  
Crystallography data of complexes **1** and **2**.

| Parameter  | <b>1</b>  | <b>2</b>   |
|--|---|--|
| Empirical formula                                | C <sub>60</sub> H <sub>92</sub> Cl <sub>4</sub> N <sub>4</sub> O <sub>10</sub> Sn <sub>4</sub>  | 2(C <sub>25</sub> H <sub>20</sub> ClNO <sub>2</sub> Sn)·C <sub>2</sub> H <sub>6</sub> O                                      |
| Formula weight                                   | 1645.94   | 1099.20  |
| Temperature (K)                                  | 297.0   | 100.0  |
| Radiation/wavelength                             | Mo K $\alpha$ /0.71073 Å  | Mo K $\alpha$ /0.71073 Å   |
| Crystal system, space group                      | Triclinic, <i>P</i> $\bar{1}$   | Orthorhombic, <i>Pbcn</i>  |
| Unit cell dimensions                             | $a = 12.2010(6)$ Å, $\alpha = 108.029(1)^\circ$<br>$b = 12.2891(6)$ Å, $\beta = 95.744(1)^\circ$<br>$c = 13.7860(7)$ Å, $\gamma = 107.168(1)^\circ$ | $a = 14.6013(3)$ Å, $\alpha = 90^\circ$<br>$b = 20.2960(5)$ Å, $\beta = 90^\circ$<br>$c = 15.8675(4)$ Å, $\gamma = 90^\circ$ |
| Volume (Å <sup>3</sup> )                         | 1835.83(16)   | 4702.30(19)  |
| Z, Calculated density (Mg/m <sup>3</sup> )       | 1, 1.489  | 4, 1.553   |
| Absorption coefficient (mm <sup>-1</sup> )       | 1.54  | 1.230  |
| <i>F</i> (000)                                   | 828   | 2208   |
| Crystal size (mm)                                | 0.43 × 0.30 × 0.21  | 0.52 × 0.25 × 0.18   |
| Crystal morphology and color                     | Block/colourless  | Block/colourless   |
| $\theta$ range for data ( $^\circ$ )             | 2.8–30.9  | 2.4–32.7   |
| Limiting indices                                 | $-17 \leq h \leq 17$ , $-17 \leq k \leq 17$ , $-19 \leq l \leq 19$  | $-21 \leq h \leq 22$ , $-24 \leq k \leq 30$ , $-24 \leq l \leq 23$   |
| Reflections collected/unique                     | 41859/11516   | 64943/8650   |
| <i>R</i> (int.)                                  | 0.027   | 0.032  |
| Completeness                                     | 98.5%   | 99.5%  |
| Max. and min. transmission                       | 0.741, 0.558  | 0.810, 0.570   |
| Goodness of fit                                  | 1.03  | 1.05   |
| $R[F^2 > 2\sigma(F^2)]$ , $wR(F^2)$              | 0.037, 0.117  | 0.024, 0.055   |
| Largest diff. peak and hole (e.Å <sup>-3</sup> ) | 1.66 and $-0.92$  | 0.52 and $-0.53$   |

**Table 2**  
Geometry parameter, bond lengths (Å) and angles (°) of complex **1**.

| Bond lengths                               |             |                                 |             |
|--|-------------|---------------------------------|-------------|
| Sn(1)–O(3)                                 | 2.039 (2)   | Sn(2)–O(3)                      | 2.0103 (19) |
| Sn(1)–C(15)                                | 2.115 (10)  | Sn(2)–C(23A)                    | 2.042 (15)  |
| Sn(1)–C(19)                                | 2.120 (8)   | Sn(2)–C(27)                     | 2.080 (16)  |
| Sn(1)–C(15A)                               | 2.13 (3)    | Sn(2)–O(4)                      | 2.115 (3)   |
| Sn(1)–O(3) <sup>a</sup>                    | 2.1505 (19) | Sn(2)–C(27A)                    | 2.153 (12)  |
| Sn(1)–C(19A)                               | 2.16 (4)    | Sn(2)–C(23)                     | 2.166 (12)  |
| Sn(1)–O(1)                                 | 2.240 (2)   | O(3)–Sn(1) <sup>a</sup>         | 2.1505 (19) |
| Bond angles                                |             |                                 |             |
| O(3)–Sn(1)–C(15)                           | 114.0 (2)   | O(3)–Sn(1)–C(19A)               | 115.1 (13)  |
| O(3)–Sn(1)–C(19)                           | 113.3 (3)   | C(15)–Sn(1)–C(19A)              | 130.8 (13)  |
| C(15)–Sn(1)–C(19)                          | 132.6 (4)   | C(19)–Sn(1)–C(19A)              | 1.8 (16)    |
| O(3)–Sn(1)–C(15A)                          | 110.8 (8)   | C(15A)–Sn(1)–C(19A)             | 134.0 (16)  |
| C(15)–Sn(1)–C(15A)                         | 3.3 (10)    | O(3) <sup>a</sup> –Sn(1)–C(19A) | 98.5 (12)   |
| C(19)–Sn(1)–C(15A)                         | 135.9 (9)   | O(3)–Sn(1)–O(1)                 | 74.34 (8)   |
| O(3) <sup>a</sup> –Sn(1)–O(3) <sup>a</sup> | 73.35 (9)   | C(15)–Sn(1)–O(1)                | 93.3 (4)    |
| C(15)–Sn(1)–O(3) <sup>a</sup>              | 98.2 (4)    | C(19)–Sn(1)–O(1)                | 96.5 (2)    |
| C(19)–Sn(1)–O(3) <sup>a</sup>              | 97.7 (3)    | C(15A)–Sn(1)–O(1)               | 93.3 (13)   |
| C(15A)–Sn(1)–O(3) <sup>a</sup>             | 96.5 (12)   | O(3) <sup>a</sup> –Sn(1)–O(1)   | 147.64 (8)  |
| C(19A)–Sn(1)–O(1)                          | 96.5(10)    | Sn(1)–C(19A)–H(19B)             | 107.1       |
| O(3)–Sn(2)–C(23A)                          | 119.5 (6)   | Sn(1)–C(19A)–H(19C)             | 107.1       |
| O(3)–Sn(2)–C(27)                           | 110.0 (6)   | C(16)–C(15)–Sn(1)               | 115.0 (6)   |
| C(23A)–Sn(2)–C(27)                         | 123.0 (8)   | Sn(1)–C(15)–H(15A)              | 108.5       |
| O(3)–Sn(2)–O(4)                            | 81.32 (9)   | Sn(1)–C(15)–H(15B)              | 108.5       |
| C(23A)–Sn(2)–O(4)                          | 107.0 (4)   | C(24)–C(23)–Sn(2)               | 116.8 (8)   |
| C(27)–Sn(2)–O(4)                           | 106.6 (5)   | Sn(2)–C(23)–H(23A)              | 108.1       |
| O(3)–Sn(2)–C(27A)                          | 109.4 (4)   | Sn(2)–C(23)–H(23D)              | 108.1       |
| C(23A)–Sn(2)–C(27A)                        | 124.0 (7)   | C(24A)–C(23A)–Sn(2)             | 115.0 (10)  |
| C(27)–Sn(2)–C(27A)                         | 1.1 (8)     | Sn(2)–C(23A)–H(23B)             | 108.5       |
| O(4)–Sn(2)–C(27A)                          | 105.6 (3)   | Sn(2)–C(23A)–H(23C)             | 108.5       |
| O(3)–Sn(2)–C(23)                           | 107.1 (3)   | C(28)–C(27)–Sn(2)               | 124.3 (13)  |
| C(23A)–Sn(2)–C(23)                         | 13.3 (6)    | Sn(1)–C(15A)–H(15C)             | 107.8       |
| C(27)–Sn(2)–C(23)                          | 136.1 (6)   | Sn(1)–C(15A)–H(15D)             | 107.8       |
| O(4)–Sn(2)–C(23)                           | 101.5 (4)   | C(20)–C(19)–Sn(1)               | 116.9 (6)   |
| C(27A)–Sn(2)–C(23)                         | 137.1 (5)   | Sn(1)–C(19)–H(19A)              | 107.6       |
| C(7)–O(1)–Sn(1)                            | 118.7 (2)   | Sn(1)–C(19)–H(19D)              | 108.7       |
| Sn(2)–O(3)–Sn(1)                           | 123.30 (9)  | Sn(2)–C(27)–H(27A)              | 106.3       |
| Sn(2)–O(3)–Sn(1) <sup>a</sup>              | 130.03 (10) | Sn(2)–C(27)–H(27D)              | 106.3       |
| Sn(1)–O(3)–Sn(1) <sup>a</sup>              | 106.65 (8)  | C(28A)–C(27A)–Sn(2)             | 115.6 (8)   |
| C(14)–O(4)–Sn(2)                           | 106.9 (2)   | Sn(2)–C(27A)–H(27B)             | 108.4       |
| Sn(1)–C(19)–H(19A)                         | 104.1       | Sn(2)–C(27A)–H(27C)             | 108.4       |
| Sn(1)–C(19A)–H(19D)                        | 109.4       |                                 |             |

<sup>a</sup> Symmetry code:  $-x + 1, -y + 1, -z + 1$ .

of the crystallography data is shown in Table 1 while the data of the bond lengths (Å) and angles (°) are listed in Table 4. The hydrogen bond geometry (Å, °) is given in Table 5 and the molecular packing diagram is depicted in Fig. S2.

Based on the crystal structure, depicted in Fig. 3, the tin atom was found to be tetra-coordinated as generally found for triphenyltin(IV) carboxylate complexes [30,52]. It is believed that the geometry occupied by the tin atom of the title complex is a distorted tetrahedral [30,52]. However, from the molecular structure diagram, the tin atom of

complex **2** was bonded to an oxygen atom (Sn–O) of the carboxylate group while the other three bonds were attributed to the bonding between the carbons of the phenyl group to the tin atom (Sn–C), resulting in the tin atom being tetra-coordinated. The bond lengths and angles of complex **2** have normal values and agree with those found for related structures [30,52].

In the crystal packing (Fig. S2), molecules are linked via intermolecular N–H...O<sub>2</sub> hydrogen bonds (Table 5) into chains propagating in [001].

The carboxylate anions were found to be chelated to the Sn(1) tin atom asymmetrically via one oxygen atom of the carboxylate group in a monodentate manner. As a result, the geometry of the Sn(1) tin atom was a highly distorted tetrahedral (Fig. 3). Moreover, based on the bond lengths (Å) and angles (°) listed in Table 5, it was found that the Sn(1)–O(2), Sn(1)–C(1), Sn(1)–C(7) and Sn(1)–C(13) bond length values were 2.1250(10), 2.1380(13), 2.1253(13) and 2.1246(15) Å, respectively, resulting in the structure being a distorted tetrahedral. Based on Table 5, the angles occupied by C(13)–Sn(1)–C(7), C(13)–Sn(1)–O(2) and O(2)–Sn(1)–C(1)

**Table 3**  
Hydrogen bond geometry (Å, °) of complex **1**.

| D–H...A                   | D–H  | H...A | D...A      | D–H...A |
|---------------------------|------|-------|------------|---------|
| N1–H1N1...O5 <sup>a</sup> | 0.79 | 2.22  | 2.986 (7)  | 166     |
| N2–H1N2...O2 <sup>b</sup> | 0.83 | 2.42  | 3.195 (8)  | 157     |
| C24–H24A...O5             | 0.99 | 2.48  | 3.312 (13) | 142     |
| C28–H28A...O5             | 0.99 | 2.57  | 3.31 (2)   | 132     |

<sup>a</sup> Symmetry codes:  $-x + 1, -y + 2, -z + 2$ .

<sup>b</sup> Symmetry codes:  $x - 1, y - 1, z$ .

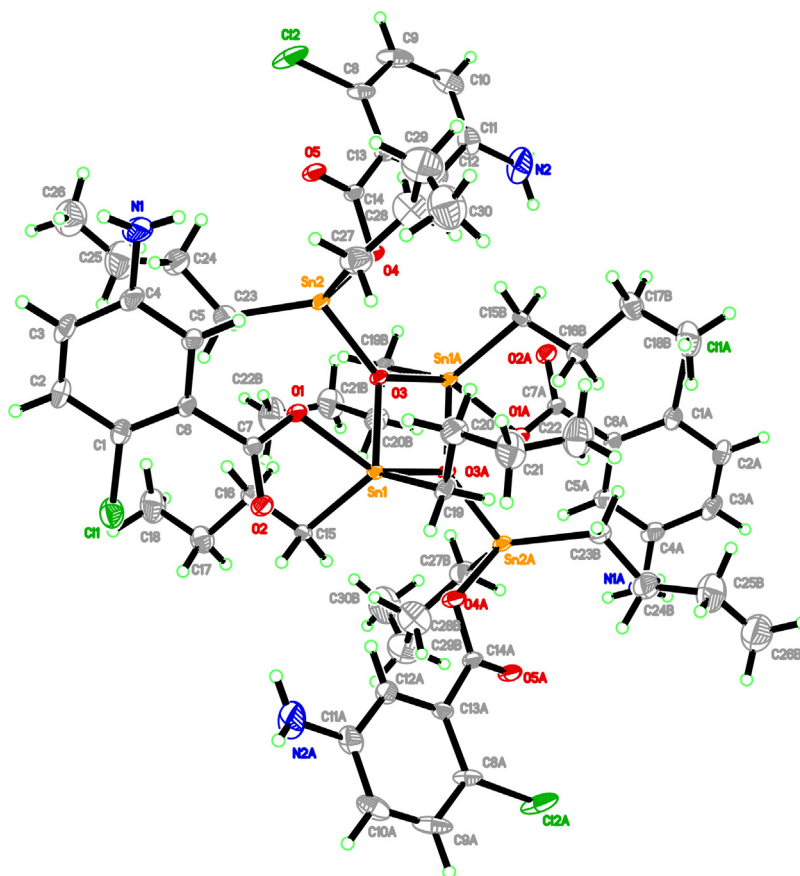


Fig. 2. (Color online.) Molecular structure of complex **1** showing 20% probability displacement ellipsoids and its atomic numbering. Minor disorder component has been omitted for clarity.

were 124.45, 98.30 and 90.11° respectively, which was the main factor attributing to the distorted tetrahedral geometry of the tin atom moiety. In addition, occurrence of one acetone molecule sandwiched in between two triphenyltin(IV) carboxylate complexes was clearly observed on the crystal structure of **2**. Referred to the similar structure documented by Yeap and Teoh in 2003 [45]; the structure obtained in 2003 was a simple monomeric type without any participation of solvent molecules. However, in the current study by altering the solvent system; an acetone molecule is participate in the crystal lattice and showed no coordination to the any tin(IV) atoms.

Based on the infrared spectral studies and the single crystal structure determination, the tin(IV) atom of **2** was tetra-coordinated and existed in a distorted tetrahedral geometry. The four bonds were attributed to the bonding of Sn–O and Sn–C, respectively. However, the NMR studies which were carried out in solution form, indicated that the tin(IV) atom of **2** was penta-coordinated and may due to the  $d_6$ -DMSO/acetone being coordinated to the tin(IV) atom. However, in crystallographic study acetone molecule was found to be present in the crystal packing but uncoordinated as shown in Fig. 2. This might be due to

different behavior of complex **2** in solvent system (NMR) and crystalline nature (single crystals).

### 3.5. *In vitro* anticancer studies

Cancer patients and mortality rate is consistently increasing worldwide because of rapid growth of world population and adoption of cancer causing behaviors specifically smoking in developing countries [53]. According to GLOBOCAN 2008 estimates, about 7.6 million cancer deaths occurred worldwide [53]. Researchers are consistently striving to explore the therapeutic ways to treat cancer. Among the different therapeutic options like chemotherapy, radiotherapy and surgery [54], Metallo-drugs in chemotherapy has recently got attention. Discovery of *cis*-platin by Rosenberg [55] and its new marketing analogues (carboplatin, lobaplatin, oxaliplatin, nedaplatin) have further created interest in metal-based anticancer drugs [1,56]. Tin complexes have been studied in detail as antibacterial agents [9,15,17–19,28] and recently against cancerous cell lines [12,26,57] other than colon cancer.

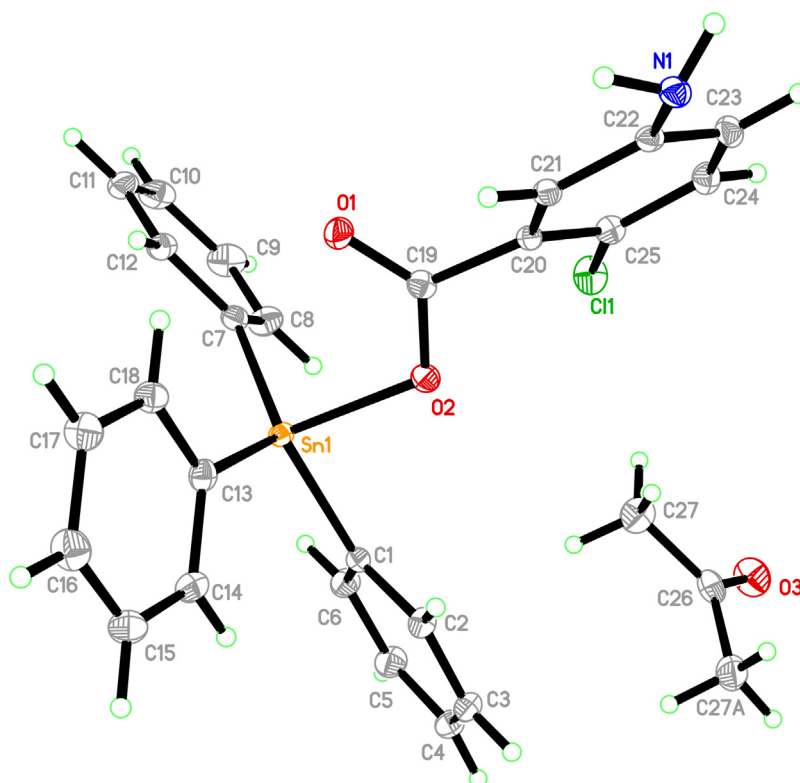


Fig. 3. (Color online.) The asymmetric unit of complex **2**, showing 50% probability displacement ellipsoids and its atomic numbering.

Table 4

Selected bond lengths (Å) and angles (°) of complex **2**.

| Bond lengths             |             |                                 |             |
|--------------------------|-------------|---------------------------------|-------------|
| Sn(1)–C(13)              | 2.1246 (14) | C(26)–C(27) <sup>a</sup>        | 1.5009 (19) |
| Sn(1)–C(7)               | 2.1253 (13) | C(27)–H(27C)                    | 0.9800      |
| Sn(1)–C(1)               | 2.1380 (13) | C(27)–H(27D)                    | 0.9800      |
| Sn(1)–O(2)               | 2.1250 (10) | C(27)–H(27A)                    | 0.9800      |
| O(3)–C(26)               | 1.2220 (3)  |                                 |             |
| C(26)–C(27) <sup>a</sup> | 1.5009 (19) |                                 |             |
| Bond angles              |             |                                 |             |
| C(13)–Sn(1)–C(7)         | 124.45 (5)  | C(14)–C(13)–Sn(1)               | 117.64 (10) |
| C(13)–Sn(1)–O(2)         | 98.30 (5)   | C(18)–C(13)–Sn(1)               | 123.25 (10) |
| C(7)–Sn(1)–O(2)          | 103.74 (4)  | O(3)–C(26)–C(27) <sup>a</sup>   | 121.68 (9)  |
| C(13)–Sn(1)–C(1)         | 112.14 (5)  | O(3)–C(26)–C(27)                | 121.67 (9)  |
| C(7)–Sn(1)–C(1)          | 118.04 (5)  | C(27) <sup>a</sup> –C(26)–C(27) | 116.65 (19) |
| O(2)–Sn(1)–C(1)          | 90.11 (4)   | C(26)–C(27)–H(27C)              | 109.5       |
| C(19)–O(2)–Sn(1)         | 114.80 (9)  | C(26)–C(27)–H(27D)              | 109.5       |
| C(6)–C(1)–Sn(1)          | 123.19 (10) | H(27C)–C(27)–H(27D)             | 109.5       |
| C(2)–C(1)–Sn(1)          | 118.52 (10) | C(26)–C(27)–H(27A)              | 109.5       |
| C(12)–C(7)–Sn(1)         | 120.62 (10) | H(27C)–C(27)–H(27A)             | 109.5       |
| C(8)–C(7)–Sn(1)          | 120.37 (10) | H(27D)–C(27)–H(27A)             | 109.5       |

<sup>a</sup> Symmetry code:  $-x + 2, y, -z + \frac{1}{2}$ .

Table 5

Hydrogen bond geometry (Å, °) of complex **2**.

| D–H...A                   | D–H        | H...A    | D...A      | D–H...A   |
|---------------------------|------------|----------|------------|-----------|
| N1–H1M1...O3 <sup>a</sup> | 0.916 (18) | 2.32(19) | 3.2177(17) | 165.3(17) |
| N1–H1N2...O2 <sup>b</sup> | 0.87(2)    | 2.24(2)  | 3.0854(16) | 163.0(18) |

<sup>a</sup> Symmetry code:  $x - \frac{1}{2}, y - \frac{1}{2}, -z + \frac{1}{2}$ .

<sup>b</sup> Symmetry code:  $-x + 1, y, -z + \frac{1}{2}$ .

In the current study, complexes **1–2** were tested against three cancerous cell lines (human colon cancer HCT 116, breast cancer MCF-7, leukemia K562) and a non-cancerous cell line (3T3-L1). The IC<sub>50</sub> values have been compiled in Table 6. Both the complexes (**1–2**) showed potential efficacies in a dose dependent manner (Fig. 4A) against HCT 116 cells with the same IC<sub>50s</sub> 0.2 μM that is about

**Table 6**  
IC<sub>50</sub> values of complexes 1–2 tested against cancerous and non-cancerous cell lines.

| Cell lines       | Carcinoma cell lines |                   |                   | Normal            |
|------------------|----------------------|-------------------|-------------------|-------------------|
|                  | HCT 116              | MCF 7             | K562              | 3T3-L1            |
| <i>Complexes</i> |                      |                   |                   |                   |
| 1                | 0.2 <sup>a</sup>     | 86.5 <sup>b</sup> | 22.9 <sup>b</sup> | 2.0 <sup>a</sup>  |
| 2                | 0.2 <sup>a</sup>     | 53.4 <sup>b</sup> | 49.6 <sup>b</sup> | 16.0 <sup>a</sup> |
| <i>Standards</i> | 5-Flourouracil       | Tamoxifen         | Betulinic acid    | Betulinic acid    |
|                  | 8.1 <sup>a</sup>     | 8.7 <sup>a</sup>  | 15.0 <sup>a</sup> | 44.0 <sup>a</sup> |
|                  | 3.7 <sup>a</sup>     | ← cis-platin →    | 3.3 <sup>a</sup>  | cis-platin        |
|                  |                      | 11.9 <sup>a</sup> |                   | 38.3 <sup>a</sup> |

<sup>a</sup> μM.  
<sup>b</sup> nM.

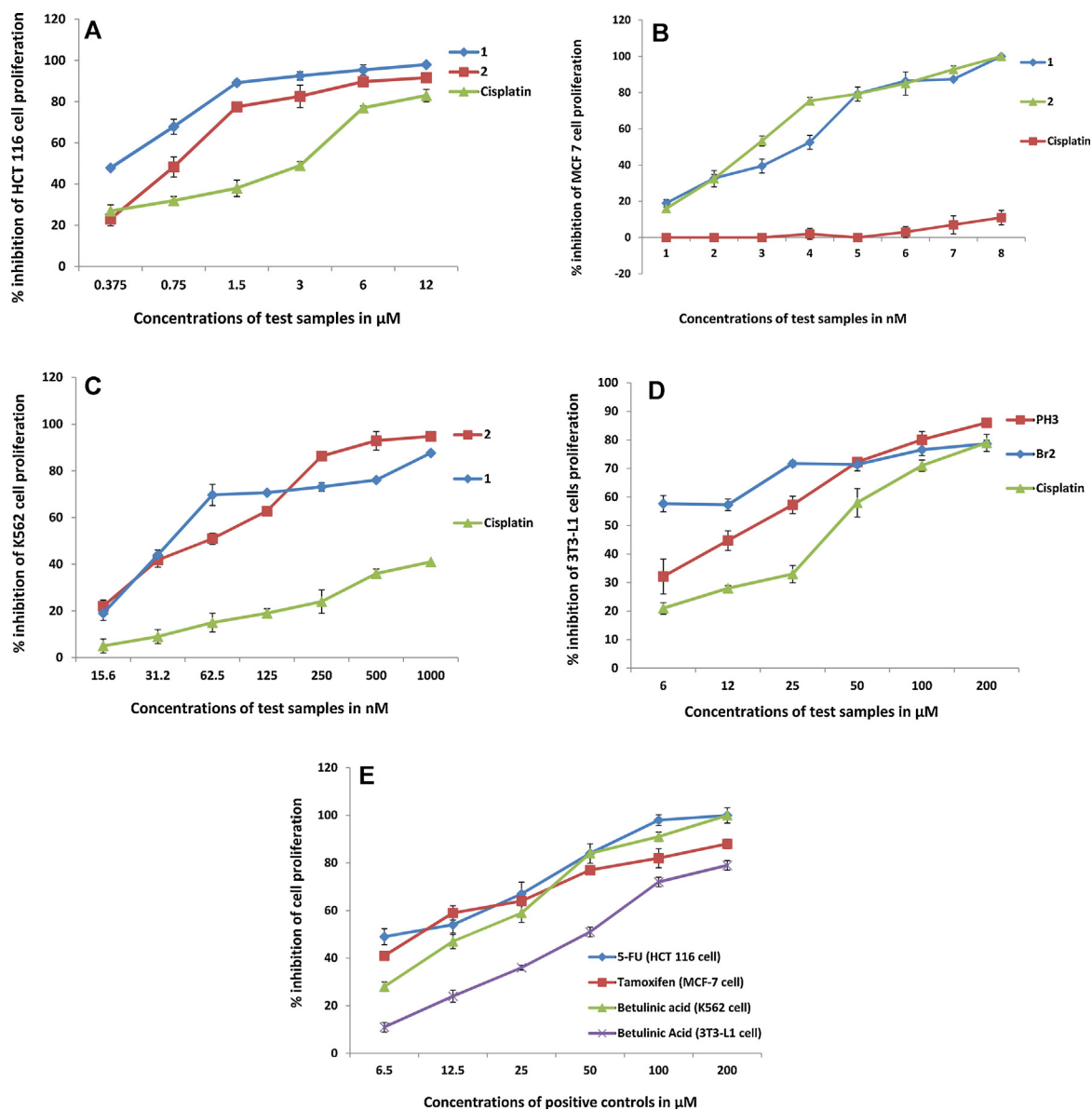


**Fig. 4.** (Color online.) A–E: The figures A–E show that the antiproliferation efficacies of cancer cell lines, HCT 116 (4A); MCF-7 (4B); K562 (4C) and a non-cancerous cell line 3T3 (4D), increased with the increase in sample concentrations in the similar manner as that for the standard drugs (4E).

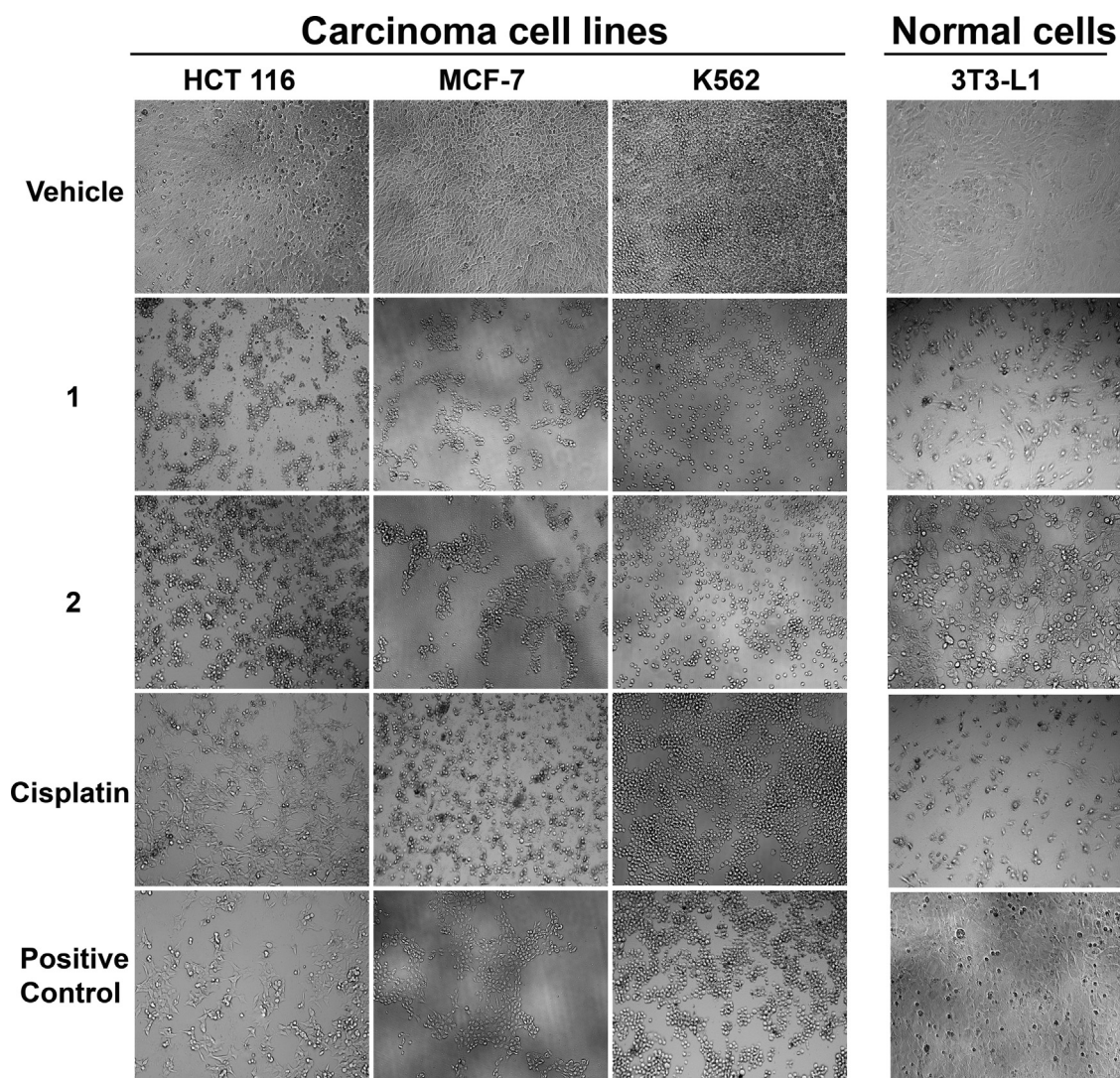


**Fig. 5.** Photomicrographic images of the cell lines, taken under an inverted phase-contrast microscope at  $\times 200$  magnification using a digital camera at 48 hours after treatment with the **1** and **2**. All the cells treated with the vehicle (0.1% DMSO) showed confluent layer of aggressively proliferating cells. Whereas, treatment with **1** showed significant ( $P < 0.01$ ) inhibitory effect on proliferation of HCT 116, MCF-7 and K562 cancer cell lines with  $IC_{50}$  0.2  $\mu$ M, 86.5 nM and 22.9 nM, respectively. The pictures revealed that the population of the treated cells is reduced drastically when compared to that of negative control. Treatment with **2** also displayed potent antiproliferative activity on HCT 116, MCF-7 and K562 cancer cell lines with  $IC_{50}$  0.2  $\mu$ M, 53.4 nM and 49.8 nM, respectively. However, both the compounds demonstrated less cytotoxicity towards normal cell line (3T3-L1), as the selective index (SI: ratio of the  $IC_{50}$  obtained from the test on normal cell (3T3-L1) versus the  $IC_{50}$  for cancer cell) was more than 10. The SI values of the compound **1** for HCT 116, MCF-7 and K562 cell lines were 10, 23 and 87, respectively. The complex **2** displayed strong antiproliferative activity as the SI values for HCT 116, MCF-7 and K562 cell lines were 84, 300 and 321, respectively. Both complexes **1** and **2** showed more pronounced antiproliferative effects than the respective standard reference drugs. The results showed that 5-fluorouracil showed significant cytotoxicity with  $IC_{50}$  8.1  $\mu$ M against HCT 116 cells. The standard reference tested against MCF-7 cells was tamoxifen, which demonstrated considerable cytotoxicity with  $IC_{50}$  8.7  $\mu$ M. Whereas, betulinic acid showed significant cytotoxicity against K562 cells with  $IC_{50}$  15.0  $\mu$ M. The use of *cis*-platin as a standard drug against all the cancerous and non-cancerous cell lines has also been included which showed inhibition values in  $\mu$ M (Table 6). *Cis*-platin induced drastic antiproliferative effect against HCT 116 and K562 cell lines compared to MCF-7 whereas remained relative safer for the normal cells (3T3-L1).

40 and 18 times better than the standard drugs (5-FU,  $IC_{50}$  8.1  $\mu$ M and *cis*-platin,  $IC_{50}$  = 3.7  $\mu$ M, respectively).

Furthermore, both the complexes showed an exceptional antiproliferation in the breast cancer (MCF-7) cells. The  $IC_{50}$  values of complexes were calculated in nanomoles (86.5 nM for **1** and 53.4 nM for **2**) which are many folds better than the respective standard drug (Tamoxifen,  $IC_{50}$  8.7  $\mu$ M and *cis*-platin,  $IC_{50}$  11.9  $\mu$ M). Similarly the complexes also showed

$IC_{50}$  values in nano moles (22.9 nM for **1** and 49.6 nM for **2**) for leukemia cell line (K562) whereas respective standard drugs (betulinic acid and *cis*-platin) showed  $IC_{50}$  values in micro moles (15.0  $\mu$ M and 3.3  $\mu$ M, respectively). This indicates that the synthesized tin complexes have many folds better anticancer activity than compared to the standard drugs tested in parallel. Also, the complexes have been tested against a normal cell line (3T3-L1) and showed

mild toxicity ( $IC_{50}$  2.0  $\mu$ M for **1** and 16.0  $\mu$ M for **2**). Complex **2** remained safer against normal cell line, however showed cytotoxicity (against cancer cells) comparable to **1**. Hence, overall complex **2** remained better than **1**. It might be due to its slower rate of releasing tin metal compared to **1**, where triphenyl could hold tin metal ion longer due to its electron withdrawing effect. It has been reported that the complexes which release metal ions at slower rate may induce better cytotoxicity in cancerous cells [1]. The standard drugs (Betulinic acid and *cis*-platin) have also been tested against the normal cells which induced a comparatively mild cytotoxicity (betulinic acid,  $IC_{50}$  44.0  $\mu$ M and *cis*-platin,  $IC_{50}$  38.3  $\mu$ M) compared to that of the cancerous cell lines. The dose dependent graphs have been shown as Fig. 4A-E and photomicrographic images of the cell lines have been presented as Fig. 5.

#### 4. Conclusion

In the current study, the complexes **1–2** have been successfully synthesized and characterized by spectroscopic techniques. The molecular structures as well as the coordination number of tin(IV) ion in **1–2** have been successfully characterized by X-ray crystallography. Both the complexes were tested against three cancerous and one non-cancerous cell lines. On the basis of results obtained, it can be concluded that tin complexes may be potential 'low dose' chemotherapeutic drugs. The fine tuning of coordinating ligands which could facilitate the slower release of metal ion in the biological system may be more feasible to further improve their efficacy. Further work on caspases to understand the pro-apoptotic potential of the reported complexes is in progress and will be reported in due course.

#### Acknowledgement

The authors would like to thank the Ministry of Higher Education of Malaysia for the Fundamental Research Grant Scheme (Project No. FRGS/1/2012/SG01/UTAR/02/1), Universiti Tunku Abdul Rahman and the Institute of Postgraduate Studies, Universiti Sains Malaysia for financial support as well as for technical assistance and facilities. Dr. Muhammad Adnan Iqbal is the recipient of a USM Postdoctoral Fellowship in research from RUI Grant No. 1001/PKIMIA/811260. The biological activity was conducted using RUT Grant No. 1001/PFARMASI/851001. The article was compiled by MAI.

#### Appendix A. Supplementary data

Supplementary data associated with this article can be found, in the online version, at <http://dx.doi.org/10.1016/j.crci.2014.06.001>.

#### References

[1] W. Liu, R. Gust, Metal N-heterocyclic carbene complexes as potential antitumor metallodrugs, *Chem. Soc. Rev.* 42 (2013) 755–773.

- [2] L. Oehninger, R. Rubbiani, I. Ott, N-Heterocyclic carbene metal complexes in medicinal chemistry, *Dalton Trans.* (2013).
- [3] G. Gasser, N. Metzler-Nolte, The potential of organometallic complexes in medicinal chemistry, *Curr. Opin. Chem. Biol.* (2012).
- [4] S.J. Tan, Y.K. Yan, P.P. Lee, K.H. Lim, Copper, gold and silver compounds as potential new anti-tumor metallodrugs, *Future Med. Chem.* 2 (2010) 1591–1608.
- [5] H. Behrmdt, A. Lunk, Biocompatibility of TiN preclinical and clinical investigations, *Mater. Sci. Eng. A* 139 (1991) 58–60.
- [6] A.L. Paschoal, E.C. Vanâncio, Canale LdCF, Silva OLd, D. Huerta-Vilca, et al., Metallic biomaterials TiN-coated: corrosion analysis and biocompatibility, *Artif. Organs* 27 (2003) 461–464.
- [7] J. Park, D.-J. Kim, Y.-K. Kim, K.-H. Lee, K.-H. Lee, et al., Improvement of the biocompatibility and mechanical properties of surgical tools with TiN coating by PACVD, *Thin Solid Films* 435 (2003) 102–107.
- [8] S. Abbas, S. Ali, M.S. Khan, M. Parvez, J. Iqbal, Synthesis, crystal structure, enzyme inhibition, DNA protection, and antimicrobial studies of di- and triorganotin(IV) derivatives of 2-thiopheneacetic acid, *J. Coord. Chem.* 66 (2013) 2765–2774.
- [9] T. Sedaghat, A. Tarassoli, Z. Ansari-Asl, H. Motamedi, Water soluble organotin(IV) complexes with Girard-T reagent-based hydrazones: synthesis, spectral characterization, and antibacterial activity, *J. Coord. Chem.* 66 (2013) 2549–2557.
- [10] A.M. Khedr, S. Jadon, V. Kumar, Synthesis, spectral analysis, and molecular modeling of bioactive Sn(II)-complexes with oxadiazole Schiff bases, *J. Coord. Chem.* 64 (2011) 1351–1359.
- [11] J. Anaconda, L. Brito, W. Pena, Cephalosporin Tin (II) complexes: synthesis, characterization, and antibacterial activity, *Synthesis and Reactivity in Inorganic, Met. Org. Nanomet. Chem.* 42 (2012) 1278–1284.
- [12] M. Khandani, T. Sedaghat, N. Erfani, M.R. Haghshenas, H.R. Khavasi, Synthesis, spectroscopic characterization, structural studies and antibacterial and antitumor activities of diorganotin complexes with 3-methoxysalicylaldehyde thiosemicarbazone, *J. Mol. Struct.* 1037 (2013) 136–143.
- [13] Y.-F. Win, S.-G. Teoh, S.-T. Ha, T.-S. Tengku-Muhammad, E. Yousif, Preliminary in vitro cytotoxic assay on HepG2 and antibacterial screening activity: synthesis and characterization of organotin (IV) complexes derivatives of 2-methyl-3-nitrobenzoic acid, *Asian J. Chem.* 25 (2013) 3376–3380.
- [14] N. Ninan, M. Muthiah, Bt. Yahaya, N.A. Park, I.-K.A. Elain, et al., Antibacterial and wound healing analysis of gelatin/zeolite scaffolds, *Colloids Surf. B Biointerf.* 115 (2014) 244–252.
- [15] B.S. Rathore, G. Sharma, D. Pathania, V.K. Gupta, Synthesis, characterization and antibacterial activity of cellulose acetate–tin (IV) phosphate nanocomposite, *Carbohydr. Polym.* 103 (2014) 221–227.
- [16] K. Sharma, S. Agarwal, S. Gupta, Antifungal, antibacterial and antifertility activities of biologically active macrocyclic complexes of tin (II), *Int. J. Chem. Tech. Res.* 5 (2013) 456–463.
- [17] A. Chilwal, P. Malhotra, A.K. Narula, Synthesis, characterization, thermal, and antibacterial studies of organotin(IV) complexes of indole-3-butylric acid and indole-3-propionic acid, *Phosphorus Sulfur Silicon Relat. Elem.* 189 (2013) 410–421.
- [18] G. Matela, R. Aman, C. Sharma, S. Chaudhary, Reactions of tin and triorganotin (IV) isopropoxides with thymol derivative: Synthesis, characterization and in vitro antimicrobial screening, *J. Serbian Chem. Soc.* (2013) 30.
- [19] M.A. Salam, M.A. Affan, M.A. Arafat, R. Saha, R. Nasrin, Synthesis, characterization, and antibacterial activities of organotin(IV) complexes with 2-acetylpyridine-N(4)-cyclohexylthiosemicarbazone (HAPCT), *Heteroatom Chem.* 24 (2013) 43–52.
- [20] R.K. Dubey, A.P. Singh, Dimeric and monomeric six-coordinate tin(IV) complexes: synthesis and spectral (IR, NMR (1H, 13C, 119Sn), TOF-MS, and ESI-MS) studies, *J. Coord. Chem.* 66 (2013) 2201–2207.
- [21] M.T. Anwar, S. Ali, S. Shahzadi, M. Shahid, Synthesis, spectroscopy, and biological activity of heterobimetallic complexes containing Sn(IV) and Pd(II) with 4-(hydroxymethyl)piperidine-1-carbodithioic acid, *Russian J. Gen. Chem.* 83 (2013) 2380–2385.
- [22] Y. Arafat, S. Ali, S. Shahzadi, M. Shahid, Preparation, characterization, and antimicrobial activities of bimetallic complexes of sarcosine with Zn (II) and Sn (IV), *Bioinorg. Chem. Appl.* (2013) 2013.
- [23] T.S. Basu Baul, A. Paul, L. Pellerito, M. Scopelliti, A. Duthie, et al., An in vitro comparative assessment with a series of new triphenyltin(IV) 2-/4-[(E)-2-(aryl)-1-diazenyl]benzoates endowed with anticancer activities: structural modifications, analysis of efficacy and cytotoxicity involving human tumor cell lines, *J. Inorg. Biochem.* 107 (2012) 119–128.
- [24] Z.-F. Chen, L. Mao, L.-M. Liu, Y.-C. Liu, Y. Peng, et al., Potential new inorganic antitumor agents from combining the anticancer traditional Chinese medicine (TCM) matrine with Ga(III), Au(III), Sn(IV) ions, and DNA binding studies, *J. Inorg. Biochem.* 105 (2011) 171–180.

- [25] Y. Li, Y. Li, X. Niu, L. Jie, X. Shang, et al., Synthesis and antitumor activity of a new mixed-ligand complex di-*n*-butyl-(4-chlorobenzohydroxamate)tin(IV) chloride, *J. Inorg. Biochem.* 102 (2008) 1731–1735.
- [26] Li Y-l, Wang Z-w, P. Guo, L. Tang, R. Ge, et al., Diorganotin(IV) derivatives of substituted *N*-hydroxybenzamides with selective cytotoxicity in vitro and potent antitumor activity in vivo, *J. Inorg. Biochem.* 133 (2014) 1–7.
- [27] O. Pellerito, C. Prinzivalli, E. Foresti, P. Sabatino, M. Abbate, et al., Synthesis, chemical characterization and biological activity of new histone acetylation/deacetylation specific inhibitors: A novel and potential approach to cancer therapy, *J. Inorg. Biochem.* 125 (2013) 16–25.
- [28] M.A. Salam, M.A. Affan, F.B. Ahmad, M.D.A. Arafath, M.I.M. Tahir, et al., Synthesis, characterization, antibacterial, and cytotoxic activities of organotin(IV) complexes derived from *N*(4)-cyclohexylthiosemicarbazone: X-ray crystal structure of [Ph<sub>2</sub>SnCl(L)], *J. Coord. Chem.* 65 (2012) 3174–3187.
- [29] R. Zhang, J. Sun, C. Ma, Structural chemistry of mononuclear, tetranuclear and hexanuclear organotin (IV) carboxylates from the reaction of di-*n*-butyltin oxide or diphenyltin oxide with rhodanine-*N*-acetic acid, *J. Organomet. Chem.* 690 (2005) 4366–4372.
- [30] Y.F. Win, S.G. Teoh, J.-J. Teh, H.-K. Fun, L. Zakaria, [4-(Diethylamino)benzoato-O] triphenyltin (IV), *Acta Crystallogr. E Struct. Rep. Online* 63 (2007) m323–m325.
- [31] Y.F. Win, S.G. Teoh, M. Vikneswaran, J.H. Goh, H.-K. Fun, Poly [[aquad-3-malonato-hexaphenylditin (IV)] acetone solvate], *Acta Crystallogr. E Struct. Rep. Online* 66 (2010) m695–m696.
- [32] Y.-F. Win, C.-S. Choong, S.-T. Ha, C.K. Quah, H.-K. Fun, (2-Chloro-4-nitrobenzoato)(methanol) triphenyltin (IV), *Acta Crystallogr. E Struct. Rep. Online* 67 (2011) m535.
- [33] M.M. Amini, A. Azadmehr, V. Alijani, H.R. Khavasi, T. Hajiashrafi, et al., Di- and triorganotin (IV) carboxylates derived from triorganotin (IV) iodide with mixed organic groups on tin: Cyclic, hexameric triorganotin (IV) carboxylates, *Inorg. Chim. Acta* 362 (2009) 355–360.
- [34] F.W. Yip, S.G. Teoh, B.M. Yamin, S.W. Ng, (Methanol-O)(2-methyl-3-nitrobenzoato-O) triphenyltin (IV), *Acta Crystallogr. E Struct. Rep. Online* 66 (2010) m1164.
- [35] D. Thorpe, A. Callejas, D. Royzman, R.D. Pike, G. Eng, et al., Synthesis and crystal structures of ionic triphenyltin complexes with oxalic and malonic acid, *J. Coord. Chem.* 66 (2013) 3647–3659.
- [36] X. Xiao, D. Du, X. Han, J. Liang, M. Tian, et al., Self-assembly of triorganotin(IV) moieties with 1,2,4,5-benzenetetracarboxylic acid: Syntheses, characterizations and influence of solvent on the molecular structure, *J. Organomet. Chem.* 713 (2012) 143–150.
- [37] Cosier Jt, A. Glazer, A nitrogen-gas-stream cryostat for general X-ray diffraction studies, *J. Appl. Crystallogr.* 19 (1986) 105–107.
- [38] G. Scheldrick, A short history of SHELX, *Acta Crystallogr. A* 64 (2008) 112–122.
- [39] R. Haque, M. Iqbal, P. Asekunowo, A.M.S.A. Majid, M. Khadeer Ahamed, et al., Synthesis, structure, anticancer, and antioxidant activity of para-xylyl linked bis-benzimidazolium salts and respective dinuclear Ag(I) *N*-heterocyclic carbene complexes (Part II), *Med. Chem. Res.* 22 (2013) 4663–4676.
- [40] R.A. Haque, N. Hasanudin, M.A. Iqbal, A. Ahmad, S. Hashim, et al., Synthesis, crystal structures, in vitro anticancer, and in vivo acute oral toxicity studies of bis-imidazolium/benzimidazolium salts and respective dinuclear Ag(I)-*N*-heterocyclic carbene complexes, *J. Coord. Chem.* 66 (2013) 3211–3228.
- [41] R.A. Haque, S.F. Nasri, M.A. Iqbal, A new dinuclear Ag(I)-*N*-heterocyclic carbene complex derived from para-xylyl linked bis-imidazolium salt: synthesis, crystal structure, and in vitro anticancer studies, *J. Coord. Chem.* 66 (2013) 2679–2692.
- [42] R.A. Haque, S.F. Nasri, M.A. Iqbal, S.S. Al-Rawi, S.F. Jafari, et al., Synthesis, characterization, and crystal structures of bis-imidazolium salts and respective dinuclear Ag (I) *N*-heterocyclic carbene complexes: in vitro anticancer studies against “human colon cancer” and “breast cancer”, *J. Chem.* (2013) 11.
- [43] M. Hussain, R. Zia Ur, M.S. Ahmad, M. Altaf, H. Stoeckli-Evans, et al., Structural and biological studies of new monomeric, tetrameric, and polymeric organotin(IV) esters of 3-(benzo[d][1,3]dioxol-4-yl)propionic acid, *J. Coord. Chem.* 66 (2013) 860–868.
- [44] G. Sandhu, S. Verma, Triorganotin (IV) derivatives of five membered heterocyclic 2-carboxylic acids, *Polyhedron* 6 (1987) 587–592.
- [45] L.-L. Yeap, S.-G. Teoh, Synthesis, spectral characterization and x-ray crystal structure of some triphenyltin (IV) carboxylate compounds, *J. Coord. Chem.* 56 (2003) 701–708.
- [46] A.C. Sau, R.R. Holmes, Characterization of phenyl-substituted penta-coordinated compounds of main group elements by <sup>1</sup>H NMR, *J. Organomet. Chem.* 217 (1981) 157–167.
- [47] M. Danish, H.G. Alt, A. Badshah, S. Ali, M. Mazhar, Organotin esters of 3-(2-furanyl)-2-propenoic acid: their characterization and biological activity, *J. Organomet. Chem.* 486 (1995) 51–56.
- [48] T.S. Basu Baul, S. Dhar, S.M. Pyke, E.R.T. Tiekink, E. Rivarola, et al., Synthesis and characterization of triorganotin(IV) complexes of 5-[(*E*)-2-(aryl)-1-diazenyl]-2-hydroxybenzoic acids.: Crystal and molecular structures of a series of triphenyltin 5-[(*E*)-2-(aryl)-1-diazenyl]-2-hydroxybenzoates (aryl = phenyl, 2-methylphenyl, 3-methylphenyl and 4-methoxyphenyl), *J. Organomet. Chem.* 633 (2001) 7–17.
- [49] J. Holeček, K. Handlír, M. Nádvořník, A. Lyčka, 13C and 119Sn NMR study of some triphenyltin(IV) carboxylates, *J. Organomet. Chem.* 258 (1983) 147–153.
- [50] J. Holeček, M. Nádvořník, K. Handlír, A. Lyčka, 13C and 119Sn NMR study of some four- and five-coordinate triphenyltin(IV) compounds, *J. Organomet. Chem.* 241 (1983) 177–184.
- [51] J. Holeček, M. Nádvořník, K. Handlír, A. Lyčka, 13C and 119Sn NMR spectra of di-*n*-butyltin(IV) compounds, *J. Organomet. Chem.* 315 (1986) 299–308.
- [52] Y.F. Win, S.G. Teoh, E.K. Lim, S.L. Ng, H.K. Fun, Synthesis, characterization and crystal structure of the bis (2, 4-dinitrobenzoato) tetrabutyl-distannoxane (IV) dimer, *J. Chem. Crystallogr.* 38 (2008) 345–350.
- [53] A. Jemal, F. Bray, M.M. Center, J. Ferlay, E. Ward, et al., Global cancer statistics, *CA Cancer J. Clin.* 61 (2011) 69–90.
- [54] M. Iqbal, R. Haque, S. Nasri, A. Majid, M. Ahamed, et al., Potential of silver against human colon cancer: (synthesis, characterization and crystal structures of xylyl (Ortho, meta, & Para) linked bis-benzimidazolium salts and Ag(I)-NHC complexes: In vitro anticancer studies), *Chem. Central J.* 7 (2013) 27.
- [55] B. Rosenberg, L. Vancamp, T. Krigas, Inhibition of cell division in *Escherichia coli* by electrolysis products from a platinum electrode, *Nature* 205 (1965) 698–699.
- [56] A. Gautier, F. Cisnetti, Advances in metal–carbene complexes as potent anti-cancer agents, *Metallomics* 4 (2012) 23–32.
- [57] L. Tian, H. Cao, S. Wang, Y. Sun, Z. Liu, Synthesis, characterization, and cytotoxic activity of tricyclohexyltin(IV) carboxylates derived from cyclic dicarboxylic anhydrides, *J. Coord. Chem.* 66 (2013) 624–637.